AIMS Energy, 5(4): 636-651.
DOI: 10.3934/energy.2017.4.636
Received: 28 April 2017
Accepted: 11 July 2017
Published: 18 July 2017

http://www.aimspress.com/journal/energy

Research article

Effect of acid leaching conditions on impurity removal from silicon doped by magnesium

Stine Espelien and Jafar Safarian *

Department of Materials Science and Engineering, Norwegian University of Science and Technology (NTNU), N-7491 Trondheim, Norway

*** Correspondence:** Email: Jafar.Safarian@ntnu.no; Tel: +474-806-1765.

Abstract: The effect of magnesium addition into a commercial silicon and its leaching refining behavior is studied for producing solar grade silicon feedstock. Two different levels of Mg is added into a commercial silicon and the leaching of the produced alloys by 10% HCl solution at 60 ℃ for different durations is performed. It is shown that the microstructure of the alloy and in particular the distribution of eutectic phases is dependent on the amount of the added Mg. Moreover, the metallic impurities in silicon such as Fe, Al, Ca and Ti are mainly forming silicide particles with different compositions. These silicides are physically more detached from the primary silicon grains and their removal through chemical and physical separation in leaching is better for higher Mg additions. It is observed that the leaching is more effective for the purification of smaller silicon particles produced from each Mg-doped silicon alloy. It is shown that acid leaching by the applied method is effective to reach more than 70% of phosphorous removal. It is also shown that the purity of silicon is dependent on the total Mg removal and effectiveness of leaching on removing the Mg_2Si phase.

Keywords: solar silicon; purification; magnesium; silicide; leaching; phosphorus

1. Introduction

The demand for solar energy has risen quickly in the recent decades, and it will continue to rise due to the global warming and energy demand. To produce solar cells, the main substrate material is

silicon, and the costs and environmental factors for the production of the silicon has an impact on making solar cells competitive against nonrenewable resources dominating the marked today. At present, the silicon for the photovoltaic (PV) industry comes mainly from the processes applied for the production of electronic grade silicon (EG-Si) and the semiconductor industry. EG-Si is produced from metallurgical grade silicon (MG-Si) through the Siemens process established in the 1950's, or the newly developed Fluid Bed Reactor (FBR) technology [1]. EG-Si is of ultra-high purity, usually above 9N (+99,9999999%), which is much higher purity than solar grade silicon (SoG-Si) of 6N purity, required in PV-devices. In the Siemens process, silicon is transformed to trichlorosilane ($HSiCl_3$) or silane (SiH_4), which is further purified and silicon is then deposited from this gas on silicon rods in bell jars. This is a very slow batch process, and it is very energy consuming to keep the bell jar hot. Regarding the production of toxic chlorine gases in the process in combination with high-energy consumption and rather low yield, this process is not environmentally friendly nor energy efficient for producing SoG-Si [1,2]. It would therefore be more convenient to produce SoG-Si through metallurgical refining route.

Several metallurgical refining techniques can be used to refine silicon, and a combination of them yields SoG-Si. One of the key techniques in all integrated metallurgical processes is *directional solidification,* where many impurities are effectively removed from silicon except phosphorous (P) and boron (B). These two elements show small segregation between solid and liquid silicon during solidification and therefore other specific processes must be employed for the removal of these impurities. For production of SoG-Si it is important that the levels of the dopants B and P are not higher than 0.3 ppmw and 0.6 ppmw, respectively. For the metallic impurities the level should be 1–10 ppmw. The main refining techniques to consider are slag refining, vacuum refining, plasma refining, gas refining, solvent refining and acid leaching [1]. Slag refining is known to be good for removal of boron from silicon, where different slag types such as $CaO\text{-}SiO_2$, $Na_2O\text{-}SiO_2$ and $CaO\text{-}Na_2O\text{-}SiO_2$ [3–6] can be used to remove B by different mechanisms. Vacuum refining is a technique that is based on the removal of impurities that have higher vapor pressure than silicon. Many of the impurities in silicon (P, Mn, Al, …) have higher vapor pressure than Si and they can be removed in reduced pressures. The thermodynamics, kinetics and mechanism of volatile elements removal from silicon in vacuum has been studied previously [7,8]. In gas refining a reactive gas is used to make volatile compounds of the impurities, in particular the removal of boron by using humidified hydrogen occurs through the formation of HBO gas [9,10]. Solvent refining is a technique that uses recrystallization from a supersaturated melt, which is depending on the segregation behaviour of the different elements in silicon. Different alloying elements such as iron [11] and aluminium [12] can be used in this process, and they affect the segregation of the impurity elements, and hence the impurities removals are dependent on the refiner metal agent.

Acid leaching as a method for silicon refining, like directional solidification, is based on the segregation of impurities between a solid silicon and a molten rich silicon phase. This leads to that the major portion of the impurities will precipitate at grain boundaries during solidification of a molten silicon. Although the leaching of solidified MG-Si will provide some purification [13,14,15], the addition of a refiner metal which yields a leachable silicide between the silicon grains is more effective and applicable for purification. In acid leaching the impurities located between the silicon grains and inside this silicide phase will be dissolved or physically separated, while the silicon

matrix will not dissolve [2,16,18]. To effectively remove the impurities, it is possible to alloy the silicon with reactive alkaline metals like calcium [17–21] and magnesium [2,9]. Inoue and co-workers alloyed silicon with calcium and leached with aqua regia, and the experiment showed a removal of boron up to 40% when 6.2% of calcium was contained in silicon [21]. The addition of Mg to molten silicon was recently studied and it was found that the best removal degree for boron is with a content greater than 2.1% Mg, and leaching with 15% HCl is more effective for dissolving of the Mg_2Si particles [2]. In other studies, where Ca was added into silicon as the refiner agent and further acid leaching was employed, it was found that leaching with HCl show significantly better results than HNO_3, H_2SO_4 and their mixtures, while applying another leaching step, before or after, with HF will improve the leaching effect on Fe-Si and Fe-Si-Ti phases [14,19]. In the present study, the effect of leaching conditions on the impurity removal from Mg-doped silicon samples with different particle sizes and durations are studied.

2. Experimental Procedure

Experimental procedure employed in the present study is described as follows.

2.1. Silicon materials

A commercial metallurgical grade silicon (MG-Si) was doped by Mg through the addition of magnesium silicide (Mg_2Si) with purity above 99% in order to reach around 2.0 and 5.0 wt% Mg in silicon. The mixture were then heated and melted in a high-density graphite crucible at 1500 ℃ in an induction furnace for 30 minutes duration at this temperature. The molten Si-Mg alloy was then slowly solidified and slowly cooled down to room temperature. The solidified silicon was crushed, and the particles were sized in desired ranges by sieving.

The two alloys were analyzed by high-resolution Inductively Coupled Plasma-Mass Spectroscopy (ICP-MS) technique and the results are shown in Table 1. The chemical composition of the MG-Si starting material is also presented in Table 1 for comparison. Alloy 1 was sieved in the size ranges: 0 to 0.315 mm, 0.315 to 1.0 mm, and 1.0 to 3.15 mm. Some of alloy 1 was also in the size range 0.15–1.0 mm for comparison to alloy 2, which was in this size range.

Table 1. The average chemical composition (ppmw) of the MG-Si and Mg-doped silicon alloys by ICP-MS.

Compound	Mg	Fe	Al	Ca	Ti	B	P	Zr	Mn	Si
MG-Si	10.2	3740.8	2772.1	165.0	340.0	47.3	16.7	13.0	81.1	balance
Alloy 1	21805.7	1879.3	643.4	375.3	157.0	47.3	12.9	6.4	39.1	balance
Alloy 2	54804.5	2154.0	1717.8	267.0	190.4	44.3	15.1	7.2	49.8	balance

2.2. Acid leaching

Crushed silicon samples were leached with hydrochloric acid (HCl) with a concentration of 15% or 10% at temperature of 60 ℃ and leaching times of 1, 3 and 5 hours. The details of the leaching conditions are given in Table 2. Each leaching trial was performed by the usage of maximum 20 ml of HCl solution with around 2 g silicon and mixing by a magnet stirrer with speed of 60 rpm. The temperature was controlled by using a thermometer with accuracy ± 1 ℃ inserted in a water bath surrounding the leaching beaker, while the required heat was supported from the bottom of the water bath, a magnetic stirrer was used to minimize the temperature profile in the bath. After leaching the particles were washed with distilled water and acetone, then they were dried at 80 ℃. In order to remove small metallic impurity particles, which are separated from silicon grains during leaching, the samples were sieved with a 50 microns sieve after drying. The samples before and after leaching were analyzed by ICP-MS technique. The analysis was done through dissolution of 20–40 mg silicon in HF + HNO_3 solution. The calibration of the results was done using blank samples and measuring the chemical composition of a reference standard silicon sample. It is worth mentioning that the ICP-MS analysis was done on two parallels and the average chemical composition was considered for data analysis.

Table 2. Applied conditions for the leaching trials.

Sample	Time [h]	Particle size [mm]	Acid concentration [vol%]	Alloy
1	1	A	15	1
2	1	B	15	1
3	1	C	15	1
4	3	A	15	1
5	3	B	15	1
6	3	C	15	1
7	5	A	15	1
8	5	B	15	1
9	5	C	15	1
10	1	D	10	1
11	3	D	10	1
12	1	D	10	2
13	3	D	10	2

A: < 0.315 mm, B: 0.315–1.0 mm, C: 1.0–3.15 mm, D: 0.15–1.0 mm.

2.3. Electron microscopy study

Metallographic samples of MG-Si, alloy 1 and alloy 2 were prepared using alloy particles with the size of around 1 cm, which were etched in an epoxy resin. Afterwards the samples were grinded and polished. Before Scanning Electron Microscopy (SEM), the samples were carbon coated to eliminate the possibility of electron charging. The microstructural analysis was performed by using Field Emission-SEM (Hitachi SU6600) supported by Energy Dispersive Spectroscopy (EDS).

3. Results and Discussion

The results of the experiments are presented and discussed as follows.

3.1. Microstructural analysis

The microstructure and phase composition of the MG-Si and the two alloys were studied in similar conditions by FE-SEM. The Back Scattered Electron (BSE) images of MG-Si, alloy 1 and alloy 2 are shown in Figures 1, 2 and 3, respectively.

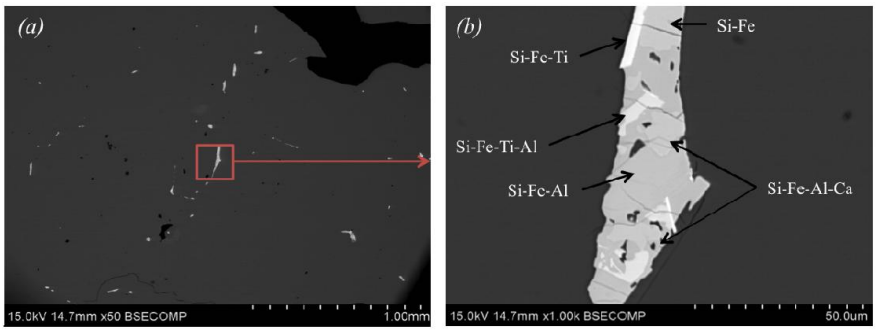

Figure 1. BSE images of MG-Si at magnifications (a): 50×, (b): 1000×.

Figure 1a shows that impurities in the MG-Si are precipitated in small non-continuous clusters between the primary silicon grains. It is not easy to distinguish the grain boundaries of the silicon here, but it is expected that these impurities are located at the grain boundaries of the primary silicon grains, due to their segregation and the lower melting point of silicide compounds than pure silicon. In Figure 1b the typical existing phases containing the impurities are shown as characterized by EDS. It is seen that all the impurities are in the form of silicides containing Fe, Al, Ca and Ti. The elements in the different phases were determined by EDS point analysis.

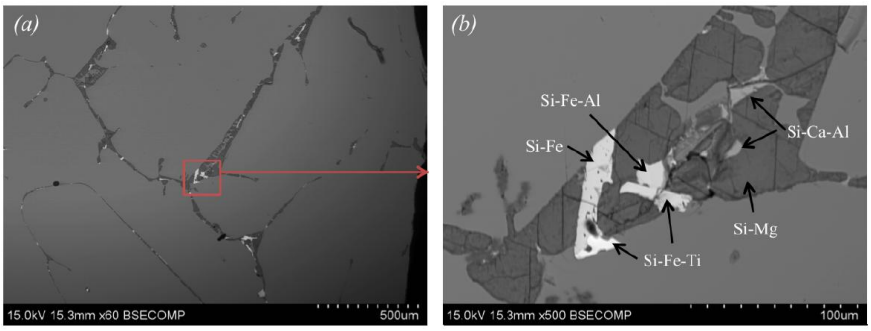

Figure 2. BSE images of alloy 1 at magnifications (a): 60×, (b): 500×.

From Figure 2a it can be seen that there is a large continuous phase of Mg_2Si between the silicon grains, and it is easily observed that the impurities are located at the grain boundaries of the

silicon grains, however in good contact with the Mg_2Si phase. In Figure 2b the existing elements in the phases are shown, and it can be seen that the initial impurities in the MG-Si are again silicides and are located mostly inside Mg_2Si phase. However, it is observed that Mg is not present in the other intermetallic phases; it is only in Mg_2Si phase.

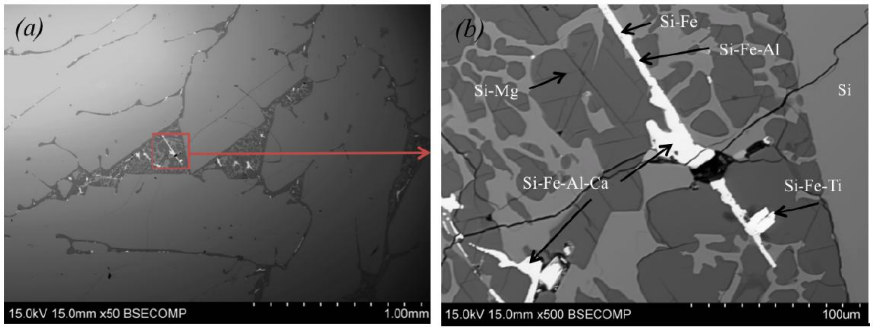

Figure 3. BSE images of alloy 2 at magnifications (a): 50×, (b): 500×.

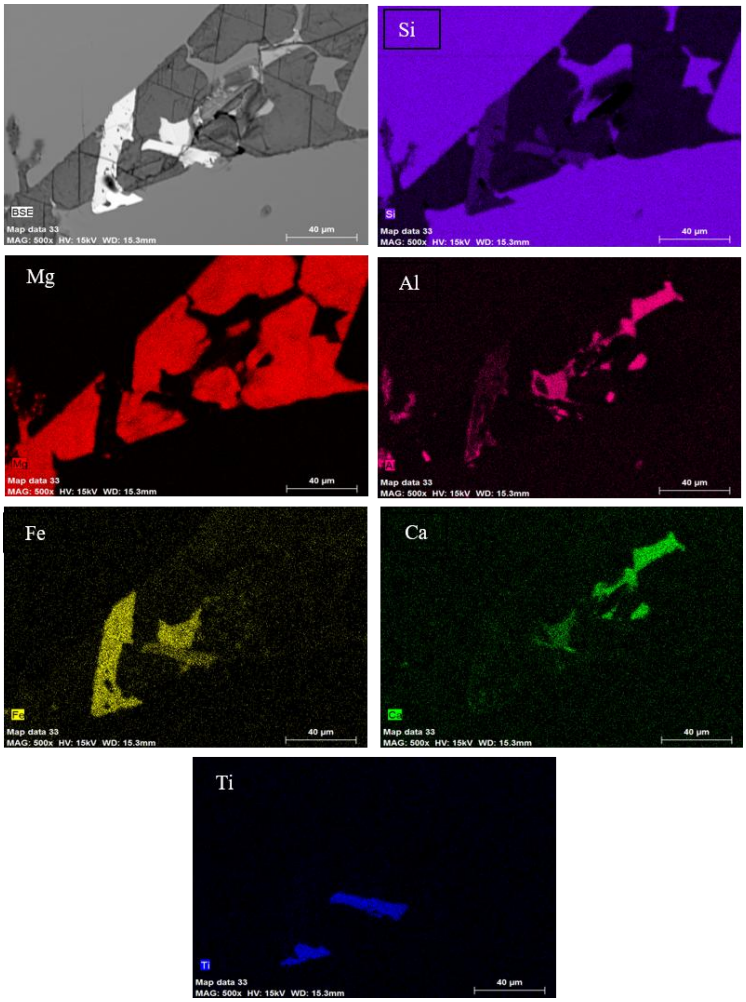

Figure 4. X-ray mapping images of silicon and the impurities in alloy 1.

The observations for alloy 2 are relatively similar to alloy 1, where the impurities are located at the grain boundaries of the primary silicon, and the impurities of the MG-Si are mostly located inside the added Mg_2Si phase. However, the metallic silicides are better embedded in Mg_2Si phase when there is more Mg in silicon as we see clearly by comparing the images in Figures 2 and 3. This may be effective for better impurity removal at high concentrations of Mg in silicon. It is worth mentioning that some small silicon particles are observed in Mg_2Si for alloy 2, and these are formed due to the eutectic reaction during solidification of the alloy, after the formation of primary silicon grains. If there is small amount of Mg present in silicon, the eutectic silicon is formed most likely on the primary silicon grains and therefore this is the main reason that we do not observe significant silicon particles in Mg_2Si in images of alloy 1 (Figure 2).

Figures 4 and 5 show the X-ray mapping images for the main impurity elements in alloys 1 and alloy 2. The figures show clearly that the added Mg is precipitated as Mg_2Si phase that is produced in the last stage of solidification through a eutectic reaction. The two images show that Al and Ca both exist in the same particles, while Fe and Ti are forming other silicide particles. However, the other silicide contains small amount of the silicide forming elements as illustrated on images in Figures 2 and 3. Figure 4 shows that silicide particles are in contact with primary silicon grains or located in the both main silicon and Mg_2Si phases. However, Figure 5 shows that the silicide particles (impurities) are more distributed in eutectic structure (Mg_2Si and eutectic fine Si particles).

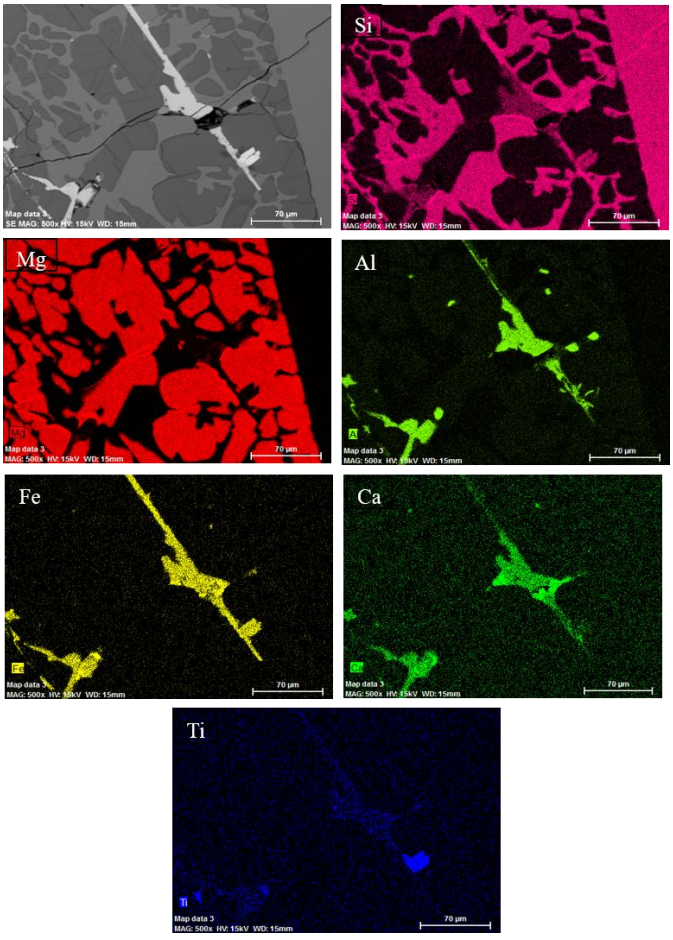

Figure 5. X-ray, mapping images of silicon and the impurities in alloy 2.

3.2. Effect of leaching conditions on silicon purification

In the present work we studied the effect of particle size and leaching time on purification of silicon. For simplification, the removal degree of each component was calculated by the following equation:

$$Removal\ degree\ (\%) = \frac{C_i - C_f}{C_i} \times 100 \quad (1)$$

Where C_i and C_f are the concentrations of impurity i in silicon before and after leaching, respectively. The initial concentrations of the impurities are obviously dependent on the particle sizes in the ranges A, B and C. The measured C_i values are given in Table 3.

Table 3. The average chemical composition (ppmw) of the alloy 1 in different particle sizes.

Size range	Mg	Fe	Al	Ca	Ti	B	P	Zr	Mn
A	28597.6	2631.5	394.3	430.2	220.4	46.5	15.9	8.5	52.8
B	19424.9	1619.3	259.8	252.2	138.4	44.9	12.2	5.5	34.6
C	12733.7	1077.2	173.0	183.1	96.4	43.2	10.9	3.7	23.8

Table 3 shows that the amount of impurities in the smaller particles is higher than the larger particles. In addition, there is significantly higher amount of Mg in the smaller particle size ranges. This indicates that the Mg_2Si phase and the impurity phases are easily separated from the silicon when the sample is crushed, and a larger amount of the impurities will be present in the smallest size range. This may be attributed to the existence of many cracks in Mg_2Si phase as clearly observed in Figures 2 and 3. The existence of these straight cracks in the Mg_2Si phase may also show that it is a brittle phase and susceptible to failure in low force. Therefore, we obtain higher concentration of Mg and other impurities in smaller particle size ranges after milling.

3.2.1. Effect of particle size

Three different particle size ranges were investigated and they where leached for 1, 3 and 5 hours. The determined removal degrees for the impurities is shown in Figure 6.

Figure 6 indicates that particle size range A has the largest removal degree above the others for all three leaching times, and for all elements. It can also be observed that the removal degrees for particle size range C are almost insignificant in 1 hour leaching time and we see only some removal of Ca, Mg and P. This may be related to the small contact area between the Mg_2Si phase and the acid for large particles. When the leaching is done for longer times as 3 and 5 hours, significant removal degrees for all impurities have risen. We may explain this observation based on the change of the size of the particles during leaching, which is due to the particles degradation through the dissolution of Mg_2Si phase between the silicon grains, which in turn provides larger reaction surface area between the acid and the main Mg_2Si phase, and also the metallic silicides. Based on this, the results for sample size C can be compared to size range A and B in long leaching time as 5 hours, but it is

still clear that this size range is the least effective upon impurity removal. We see that size range B shows results close to size range A, and it is therefore believed that a small size range is the most efficient for removal of impurities with regard to the mechanism explained above. Obviously, decreasing the size of silicon before leaching has limitation regarding the recovery of silicon. Firstly, when the particles are washed after leaching, the smallest particles will be flocculent, and not settle and separated from the solution. Secondly, in the removal of fine undissolved intermetallic particles by sieving after leaching, a larger amount of the fine silicon particles will also be sieved out. Therefore, there must be an optimum particle size for a given optimum process condition to reach the highest removal degree and silicon yield. It is worth mentioning that, the loss of silicon was not significant for particle size range B and C, while for A some loss was observed, but the amount was not measured.

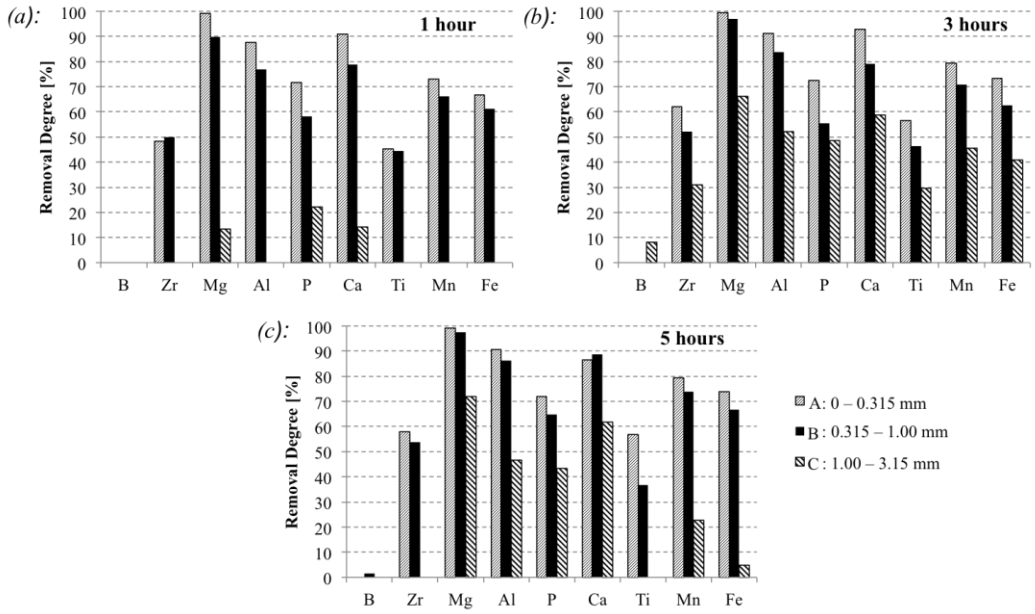

Figure 6. The removal degree of impurities from alloy 1 particles with different sizes leached for different times.

3.2.2. Effect of leaching time

As mentioned before, the effect of leaching time was studied on all the three particle size ranges. The results for particle size range A are presented in Figure 7 for more clear discussion, and for the other sizes the results can be found in Figure 6.

It is seen that the removal degrees of impurities are increased with leaching time for all impurities up to 3 hours leaching time, while for a few elements (Zr and Ca) the removal degree is lower after 5 hours. The reason for this is most probably due to the very small segregation coefficients of these elements [16] and their concentration in localized positions between the silicon grains. For the sample size range B, however, it was observed that almost all impurities show removal degrees that increased up to 5 hours leaching time. The provided information in Figure 7

indicate that the leaching process is a fast process and a large extent of impurity removal occurs in shorter times than 1 hour. Therefore, in order to study the kinetics of the process more precisely and determine the reaction kinetic parameters, working in short leaching durations is required.

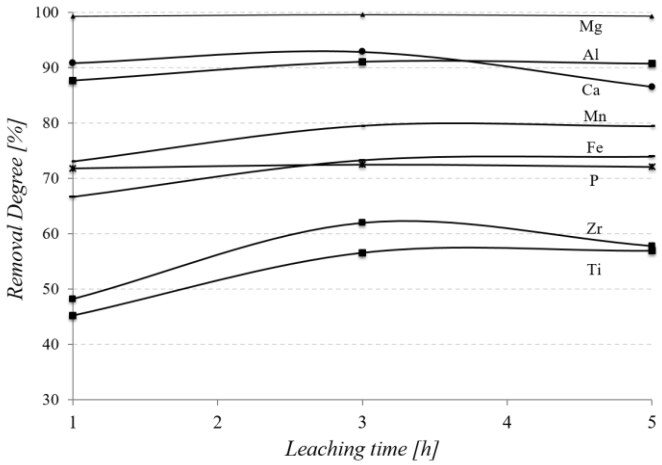

Figure 7. Removal degree for different impurities in alloy 1 with particle size range A after 1, 3 and 5 hours leaching time.

3.2.3. Effect of magnesium content in the alloy

In the present work, two Mg-containing silicon samples were studied (alloys 1 and 2). They were leached for 1 and 3 hours at 60 °C and with the use of 10% HCl for the particle size of 0.15–1.00 mm. The impurity contents in the samples after leaching are shown in Figure 8, and the removal degrees of elements in different durations are shown in Figure 9.

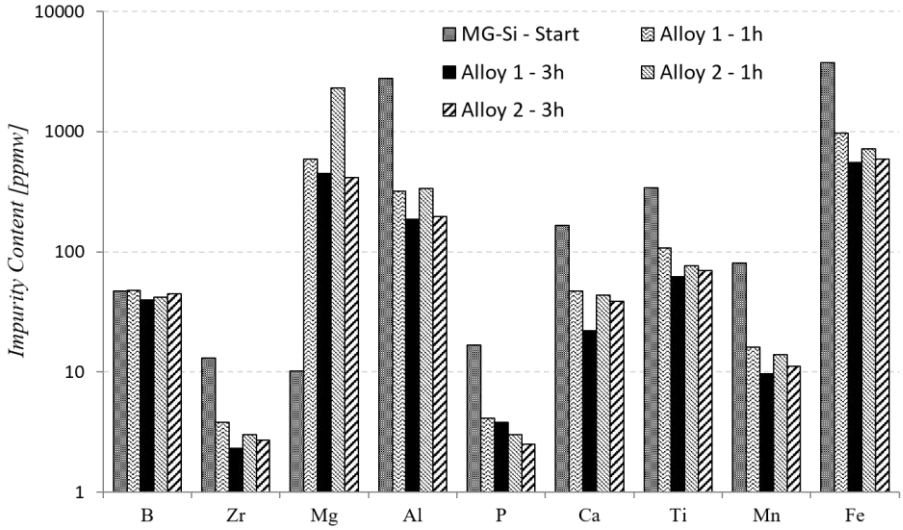

Figure 8. Impurity contents in leached alloys 1 and 2 within 1 and 3 hours, the concentrations of elements in the MG-Si is also presented.

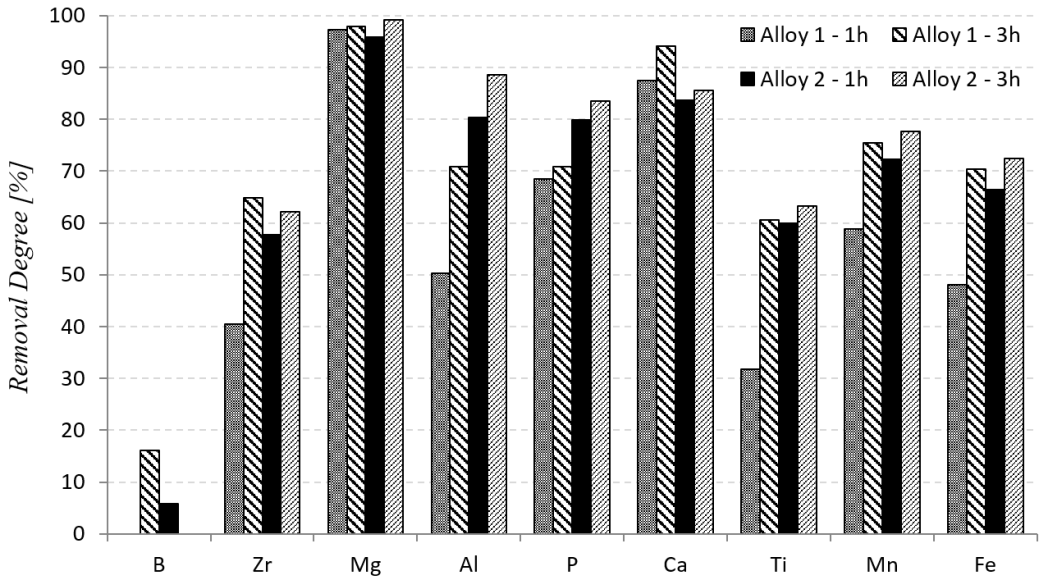

Figure 9. Removal degree of the impurities in leached alloys 1 and 2 within 1 and 3 hours.

From Figure 8 it can be seen that for both alloy 1 and 2, the impurity contents are reasonably lower than the initial MG-Si starting material, except for boron. The removal of B is not significant due to its large distribution coefficient between solid and liquid silicon during solidification; during the formation of primary silicon grains. It is observed that the removal of impurities is better for the sample doped with higher amount of Mg; alloy 2. The removal of impurities from alloy 2 is better than alloy 1 due to the better distribution of the metallic silicide in contact with Mg_2Si phase in alloy 2 compared to alloy 1 so that in leaching these particles are more efficiently removed by the dissolution of Mg_2Si phase. The effect of total Mg content on the removal of impurities (silicide particles) is schematically illustrated in Figure 10. As we see in this figure, the possibility of the removal of impurities is more favorable at higher Mg concentration. However, if the concentration of Mg in the alloy (the added Mg) is high, it may cause lower silicon yield due to the formation of more fine eutectic silicon particles in Mg_2Si phase. According to Figure 10, the chance of metallic impurities to be lock in primary silicon grain is decreased by the addition of more Mg and they are better dissolved or detached from silicon grains in leaching.

The low concentrated impurities such as P, B, Mn,…are removed in leaching due to the dissolution of Mg_2Si and also removal of silicide particles. It is expected that the metallic impurities are mostly in the silicide phases, while P is most likely in combination with the Mg and Ca containing phases. These two elements are making more stable phosphides than other existing impurities and therefore it is expected to have P in the form of Mg_3P_2 or Ca_3P_2, mainly in contact with Mg_2Si phase. The better removal of P from alloy 2 than alloy 1 for a given leaching time may be due to the formation of fine particles of these phases in Mg_2Si phase.

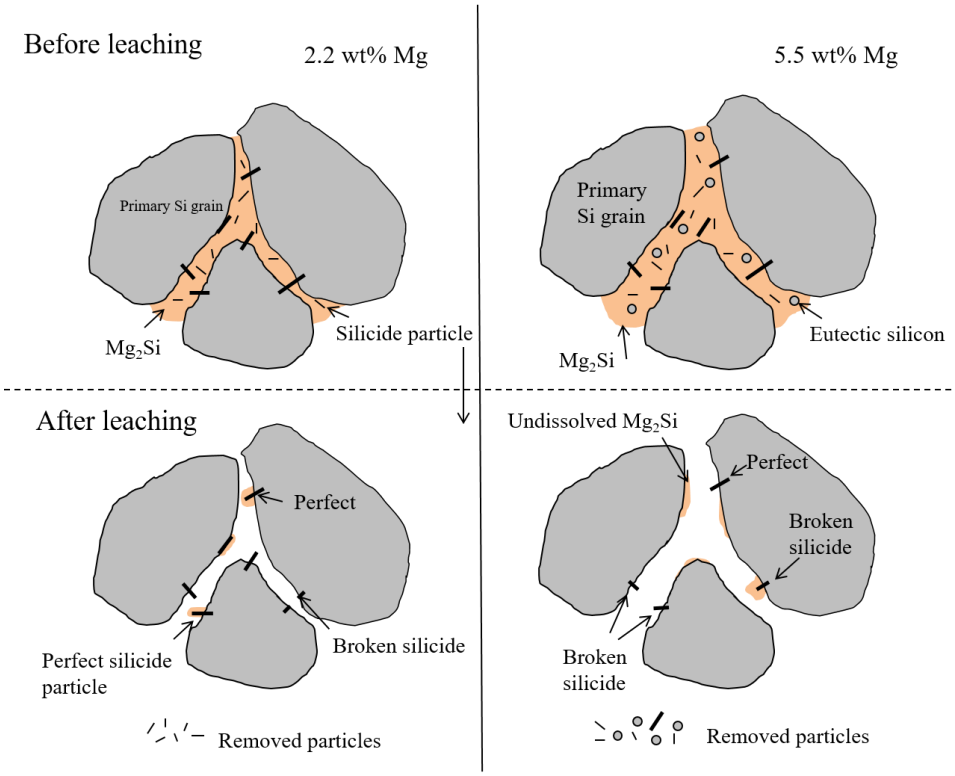

Figure 10. Schematic of leaching process for two Mg containing silicon alloys and the mechanism of impurities removal.

3.3. Effect of overall Mg removal by leaching

In order to study the effect of the overall Mg removal by leaching, the removal degrees of the different impurities against the total Mg removed from alloy 1 can be studied as shown in Figure 11. The results presented here are from trials #4 to #9 shown in Table 2. In addition, the effect of Mg removal on the silicon purity is shown in Figure 12, based on the results of trials #1 to #9 in Table 2.

In Figure 11 it can be seen that P and Al removal degrees show a good approximate linear dependency on Mg removal degree, while for Ca and Fe this approximation is less linear. For P one of the reasons can be that P is bounded to the Mg_2Si phase, and not with the silicides. Due to this, the removal of P is closely bounded to the Mg removal. The microstructural study shows that Al, Ca and Fe are appeared in the form of silicides and their silicide intermetallic particles can be completely or partly located in the Mg_2Si phase as clearly seen in Figures 2 to 5. For Al that is found as a silicide located together with the other silicides as shown in figure 4, and so the mechanism of its removal will not be the same. Since Ca and Fe do not follow the similar linear dependency as P and Al, we may say that the aluminum containing silicides are either more soluble than Fe and Ca in the acid, or they are more easier physically removed than these elements. For Ca the solubility in the acid is believed to be high, and hence the less linear behavior must be affected by other conditions. For Fe containing silicides, the solubility in the acid is lower, and hence this element is more dependent on physical separation, which happens better in higher total Mg removal; more leaching of Mg_2Si.

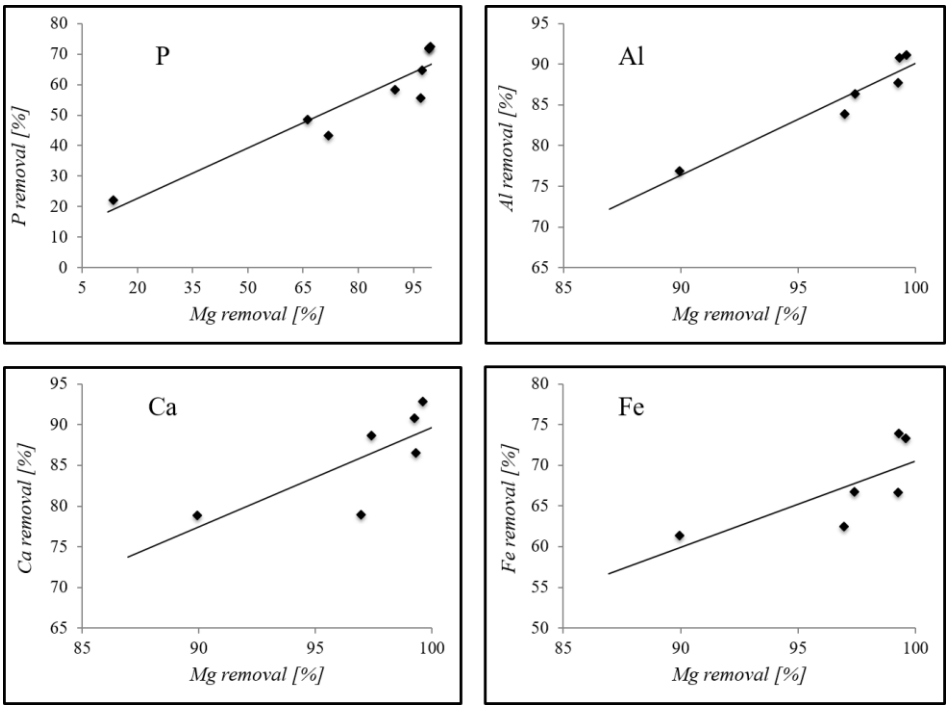

Figure 11. The relationship between removals of the impurities: P, Al, Ca, Fe, and the total Mg removal.

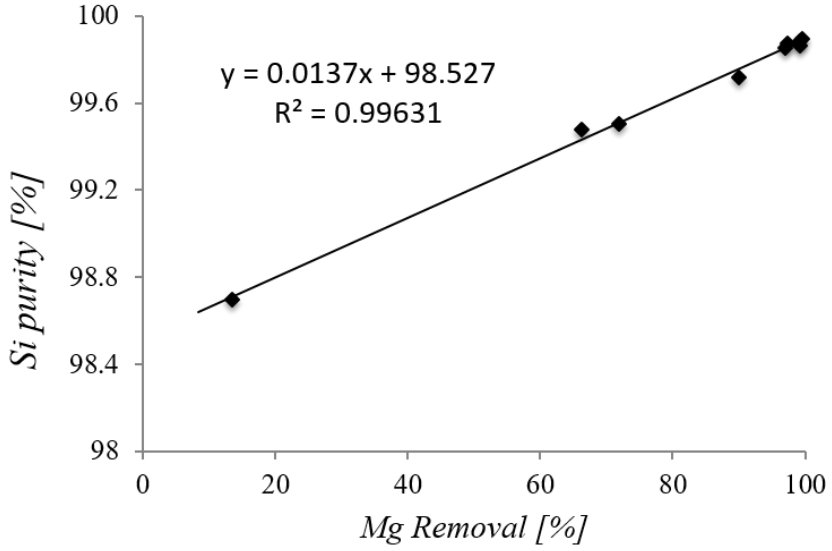

Figure 12. The relationship between silicon purity and Mg removal degree.

Based on the information we obtain from Figure 11, the purity of silicon is dependent on Mg removal degree. Figure 12 shows the measured silicon purities as a function of Mg removal degree with a linear relationship. The obtained linear regression line in the figure with a fitting close to unity shows the silicon purity dependency on total Mg removal. This indicates that optimizing the leaching

conditions to remove as much as possible of the Mg is the key issue for obtaining the highest purification degree.

3.4. Silicon yield

Regarding the above-discussed mechanism for the removal of the impurities, the silicon particles forming through the eutectic transformation are partially distributed in the Mg_2Si phase and they are removed through the leaching. This is obviously occur more for the higher Mg concentrations in the solidified Si-Mg alloy as schematically shown in Figure 10. If Mg_2Si is used for doping of silicon, as for the majority of experiments in the present study, the maximum silicon loss may therefore be calculated as the amount of eutectic silicon. For the leached alloys 1 and 2 we may calculate the maximum silicon losses as 1.6% and 4.04% were calculated by employing the lever rule.

4. Conclusion

A commercial silicon was doped with Mg and two alloys of about 2 wt% and 5 wt% Mg were produced. The microstructure of the alloys and their leaching behavior were studied and the following conclusions have been obtained:

(1) The main impurities are in the form of silicide particles, and they are located partially or completely inside the Mg_2Si eutectic phase.
(2) Smaller sized crushed Si-Mg alloy particles show better purification by leaching.
(3) The rate of impurity removal is fast and large extent of impurity removal is obtained within 1 hour leaching time, the removal degree of impurities in longer times is minimally increased.
(4) Si doped by higher amount of Mg (5 wt% Mg) shows better purification than silicon doped by less Mg (2 wt% Mg) in leaching. However, higher amount of Mg will cause lower silicon yield due to greater formation of eutectic silicon trapped inside the Mg_2Si phase.
(5) Some elements like P and Al show good linear removal relationship with the Mg removal in leaching, while for Ca and Fe less linear dependency is observed.
(6) The removal of impurities by leaching is dependent on their existence in silicides and also their physical contact with the leachable Mg_2Si phase.
(7) The silicon purity shows linear relationship with the overall Mg removal.

Acknowledgement

The authors appreciate the financial support of this study through the Research Domain 3-refining and recycling of SFI-metal production (Norwegian acronym for Centre for Research driven Innovation (CRI)). The Support from Norwegian FME Sustainable Solar Cell Technology is also appreciated.

Conflict of Interest

All authors declare no conflicts of interest in this paper.

References

1. Safarian J, Tranell G, Tangstad M (2012) Processes for upgrading metallurgical grade silicon to solar grade silicon. *Energy Procedia* 20: 88–97.
2. Safarian J, Tranell G (2016) Silicon purification through magnesium addition and acid leaching, In: 32nd European Photovoltaic Solar Energy Conference and Exhibition, 1011–1014.
3. Wu JJ, Long LY, Ma WH, et al. (2014) Boron removal in purifying metallurgical grade silicon by CaO-SiO_2 slag refining. *Trans Nonferrous Met Soc China* 24: 1231–1236.
4. Jakobsson LK (2013) Distribution of boron between silicon and CaO-SiO_2, MgO-SiO_2, CaO-MgO-SiO_2 and CaO-Al_2O_3-SiO_2 slags at 1600 ℃. *Mat Sci Eng* 2013: 326.
5. Safarian J, Tranell G, Tangstad M (2013) Thermodynamic and kinetic behavior of B and Na through the contact of B-doped silicon with Na_2O-SiO_2 slags. *High Temp Mater Proc* 44: 571–583.
6. Safarian J, Tranell G, Tangstad M (2015) Boron removal from silicon by CaO-Na_2O-SiO_2 ternary slag. *Metall Mater Trans E* 2: 109–118.
7. Safarian J, Tangstad M (2012) Kinetics and mechanism of phosphorus removal from silicon in vacuum induction refining. *Metall Mater Trans B* 31: 73–81.
8. Safarian J, Tangstad M (2012) Vacuum refining of molten silicon. *Metall Mater Trans B* 43: 1427–1445.
9. Safarian J, Tang K, Hildal K, et al. (2014) Boron removal from silicon by humidified gases. *Metall Mater Trans B* 1: 41–47.
10. Safarian J, Tang K, Olsen JE, et al. (2014) Mechanisms and kinetics of boron removal from silicon by humidified hydrogen. *Metall Mater Trans B* 47: 1–17.
11. Esfahani S (2010) Solvent refining of metallurgical grade silicon using iron. Master thesis of applied science at University of Toronto. Available from: https://tspace.library.utoronto.ca/bitstream/1807/25570/3/Shaghayegh_Esfahani_201011_MASc_thesis.pdf.
12. Mohanty BC, Galgali RK (1987) Solvent refining of metallurgical grade silicon. *Sol Energ Mat* 16: 289–296.
13. Dietl J (1983) Hydrometallurgical purification of metallurgical grade silicon. *Solar Cells* 10: 145–154.
14. Santos IC, Gonçalves AP, Santos CS, et al. (1990) Purification of metallurgical grade silicon by acid leaching. *Hydrometallurgy* 23: 237–246.
15. He F, Zheng S, Chen C (2012) The effect of calcium oxide addition on the removal of metal impurities from metallurgical-grade silicon by acid leaching. *Metall Mater Trans B* 43: 1011–1018.

16. Espelien S, Tranell G, Safarian J (2017) Effect of magnesium addition on removal of impurities from silicon by hydrometallurgical treatment. *Energy Technology 2017, Carbon Dioxide Management and Other Technologies*, Springer International Publishing, 355–365.
17. Shimpo T, Yoshikawa T, Morita K (2004) Thermodynamic study of the effect of calcium on removal of phosphorus from molten silicon by acid leaching treatment. *Metall Mater Trans B* 35: 277–284.
18. Yu ZL, Ma WH, Dai YN, et al. (2007) Removal of Iron and aluminium impurities from metallurgical grade-silicon with hydrometallurgical route. *Trans Nonferrous Met Soc China* 17: 1030–1033.
19. Jian Z, Li T, Ma X, et al. (2009) Optimization of the acid leaching process by using ultrasonic field for metallurgical grade silicon. *J Semiconductors* 30: 22–27.
20. Juneja JM, Mukherjee TK (1986) A study of the purification of metallurgical grade silicon. *Hydrometallurgy* 16: 69–75.
21. Inoue G, Yoshikawa T, Morita K (2003) Effect of calcium on thermodynamic properties of boron in molten silicon. *High Temp Mat Proc* 22: 221–226.

AIMS Press